Lurbinectedin (PM01183), a New DNA Minor Groove Binder, Inhibits Growth of Orthotopic Primary Graft of Cisplatin-Resistant Epithelial Ovarian Cancer

August Vidal [4 ‡], Clara Muñoz [1‡], María-José Guillén [2], Jemina Moretó [3], Sara Puertas [1], María Martínez-Iniesta [1], Agnés Figueras [1], Laura Padullés [1], Francisco J. García-Rodriguez [1], Mireia Berdiel-Acer [1], Miguel A Pujana [1], Ramón Salazar [5], Marta Gil-Martin [5], Lola Martí [6], Jordi Ponce [6], David G Molleví [1], Gabriel Capella [1], Enric Condom [4], Francesc Viñals [1], Dori Huertas [3], Carmen Cuevas [2], Manel Esteller [3], Pablo Avilés [2*] and Alberto Villanueva [1*]

1. Translational Research Laboratory, Catalan Institute of Oncology - Bellvitge Biomedical Research Institute (IDIBELL), 08907 L'Hospitalet de Llobregat, Barcelona, Spain.
2. Department of Research and Development (R&D), PharmaMar S.A., 28770 Colmenar Viejo, Madrid, Spain.
3. Cancer Epigenetics and Biology Program (PEBC), Bellvitge Biomedical Research Institute (IDIBELL), Barcelona, Catalonia, Spain.
4. Department of Pathology, Hospital Universitari de Bellvitge - IDIBELL.
5. Department of Medical Oncology, Catalan Institute of Oncology - IDIBELL.
6. Department of Gynecology, Hospital Universitari de Bellvitge - IDIBELL.

Running Title: Lurbinectedin inhibits growth of ovarian cancer

‡ These authors contributed equally to this work

* Corresponding authors

Alberto Villanueva, Ph.D.: Laboratory of Translational Research, Catalan Institute of Oncology - Bellvitge Biomedical Research Institute (IDIBELL), Hospital Duran i Reynals, Avda Gran Via s/n km 2.7, L'Hospitalet de Llobregat, 08907 Barcelona, Spain.
Telephone: +34 93 260 79 52; Fax: +34 93 260 74 66
avillanueva@iconcologia.net

Pablo Aviles, Pharm. D., Ph.D.: Department of Research and Development, PharmaMar S.A., Avda. de los Reyes, 1, Polígono Industrial La Mina, 28770 Colmenar Viejo, Madrid, Spain.
Telephone: +34 91 823 45 14; Fax: +34 91 823 45 06.
paviles@pharmamar.com

Abstract

Purpose: Epithelial ovarian cancer (EOC) is the fifth leading cause of death in women diagnosed with gynecological malignancies. The low survival rate is due to its advanced-stage diagnosis and either intrinsic or acquired resistance to standard platinum-based chemotherapy. So, the development of effective innovative therapeutic strategies to overcome cisplatin resistance remains a high priority.

Experimental Design: To investigate new treatments in *in vivo* models reproducing EOCs tumor growth, we generated a preclinical model of ovarian cancer after orthotopic implantation of a primary serous tumor in nude mice. Further, matched model of acquired cisplatin-resistant tumor version was successfully derived in mice. Effectiveness of lurbinectedin (PM01183) treatment, a novel marine-derived DNA minor groove covalent binder, was assessed in both preclinical models as a single and a combined-cisplatin agent.

Results: Orthotopically perpetuated tumor grafts mimic the histopathological characteristics of primary patients' tumors and they also recapitulate in mice characteristic features of tumor response to cisplatin treatments. We demonstrated that single lurbinectedin or cisplatin combined therapies were effective in treating *cisplatin-sensitive* and *cisplatin-resistant* preclinical ovarian tumor models. Furthermore, the strongest *in vivo* synergistic effect was observed for combined treatments, especially in cisplatin-resistant tumors. Lurbinectedin tumor growth inhibition was associated with reduced proliferation, increased rate of aberrant mitosis and subsequent induced apoptosis.

Conclusions: Taken together, preclinical orthotopic ovarian tumor grafts are useful tools for drug development, providing hard evidence that lurbinectedin might be a useful therapy in the treatment of epithelial ovarian cancer by overcoming cisplatin resistance.

Translational Relevance

The efficacy of conventional platinum-based chemotherapy for EOCs is limited; most patients show an initial response to treatment but upon relapse, the platinum response rates progressively diminish and they ultimately die. So, the development of effective innovative therapeutic strategies to overcome cisplatin resistance remains a high priority. On the way to identifying novel therapeutic targets and for drug testing we have developed two paired (*cisplatin-sensitive* and *cisplatin-resistant*) preclinical models of serous carcinoma phenocopying patients' primary tumor features including chemotherapy response behavior. In this study we demonstrate that single lurbinectedin (PM01183), a novel marine-derived DNA minor groove covalent binder, or cisplatin combined therapies were effective in treating *cisplatin-sensitive* and *cisplatin-resistant* preclinical models. Thus we present hard evidences that lurbinectedin might be a useful therapy in epithelial ovarian cancer overcoming acquired cisplatin resistance providing a rationale for future trials.

Introduction

Ovarian cancer is the fifth leading cause of death among women, and is the most common cause arising from gynecological malignancies (1). Although progress has been made in the treatment of epithelial ovarian cancer (EOC) by improved surgical debulking and the introduction of platinum-taxane regimens, overall five-year survival is only 29% in advanced-stage disease (2-6). This low survival rate is due to its frequent diagnosis at an advanced stage and by intrinsic and acquired resistance to platinum-based chemotherapy. In the recurrent disease setting, those patients who experience progression through first-line, platinum-based therapy (*platinum-refractory*), or those who experience relapse within six months of receiving platinum therapy (*platinum-resistant*) are typically treated with a second-line non-platinum-based regimen, such as single-agent doxorubicin (7) gemcitabine (8), paclitaxel, topotecan (9), vinorelbine (10) or trabectedin plus pegylated liposomal doxorubicin (11). Agents yielding responses in the range of 15-20% that last a median of approximately four months, emphasize the great need for novel effective therapeutic strategies for its management (12-15).

DNA structure features two well-defined clefts known as the major and minor grooves, and DNA-binding proteins and drugs usually make contacts with the sides of the bases exposed in both grooves (16, 17). The DNA major groove is a site of attack for cisplatin and many alkylating agents, and when cisplatin binds to DNA three types of lesions can be formed on purine bases: monoadducts, and intra- and interstrand crosslinks. On the other hand, other anti-tumor drugs including mitomycin C, chromomycin A_3 and ecteinascidins, bind to the minor groove (18). One of the best examples is trabectedin (Yondelis®), which reacts with certain guanines in the minor groove of DNA to form a covalent bond (19-21). The adduct is stabilized by van der Waals interactions with nucleotides in the opposite DNA strand, creating the equivalent of a functional interstrand crosslink (22). Lurbinectedin (PM01183) is a new synthetic alkaloid that is structurally related to ecteinascidins (23), which, with the exception of a module addition (ring C), confer important pharmacokinetic and pharmacodynamics properties benefits as well intrinsic activity (24-26).

Establishment of preclinical models phenocopying patients' primary tumor features, which accurately reflect phenotypic, genotypic and tumor chemotherapy response behavior, is a basic step on the way to identifying novel therapeutic targets and for testing novel treatments (27, 28). Several lines of evidence indicate that engrafting primary tumor tissues orthotopically into immune-deficient mice (termed "tumor grafts") may be outstandingly valuable preclinical models for new drug development, and for reducing the high failure rate that exists in translating preclinical results to patients (29-33).

Here we report the establishment and characterization of a serially transplantable, orthotopic, subject-derived epithelial ovarian tumor graft that retains crucial characteristics of the original primary tumor specimen, and its further development as an *in vivo* cisplatin-resistance

tumor model. We demonstrate in engrafted pre-clinical models that lurbinectedin, a new minor groove DNA binder, is effective in the treatment of experimental ovarian tumors as a single or a combined-cisplatin agent. Overall, we present evidence of the efficacy of a therapeutic strategy based on the idea that a combination of two drugs that bind differentially to each DNA groove could overcome frequent cisplatin resistance in advanced-stage ovarian cancer.

Results

Orthotopic model of epithelial ovarian cancer mimics the histopathological characteristics of primary patients' tumors.

Primary tumors engrafted in the ovarian surface of athymic female mice (named OVA1X) grew as large solid masses. Ovarian infiltration and neighboring organ invasion or ascitis were not seen in any of the implanted animals (**Fig 1A**). The engrafted rate was close to 95% in all mouse-to-mouse passages, with a mean time of *ca.* 1000 to 1500 mm^3 during the first six passages of 84 ± 8 days. As shown in **Fig 1A**, a very high histological correlation was found between primary and engrafted tumors. Indeed, OVA1X had a typical serous adenocarcinoma appearance showing high cellularity, cellular papillae formation and irregular slit-like spaces, and it remained stable throughout multiple rounds of serial mouse-to-mouse transplantation. Ki-67 immunostaining revealed a similar proliferative rate in primary and engrafted tumors, and they both preserved the same cytokeratin 7 (CK7) and Wilm's tumor susceptibility gene 1 (WT1) immunostaining pattern. Engrafted OVA1X tumor also retained their levels of positive immunostaining for estrogen receptor through mouse-to-mouse passages. Ascitis or synchronic peritoneal implants arising through tumor perpetuation were rarely identified in mice (data not shown).

Cisplatin treatment of engrafted tumor recapitulates characteristic features of primary tumor response in mice.

OVA1X-implanted mice were treated with low (2 mg/kg), intermediate (3.5 mg/kg) and high (5 mg/kg) doses of cisplatin, and short- and long-term responses were evaluated (**Fig 1B**). Low or intermediate doses of cisplatin were associated with a good short-term response, characterized by significant tumor weight reduction relative to the control group, whilst there was a complete response at high doses. Long-term response was investigated in a subgroup of mice (n=4-6 mice/treatment/dose) that were kept alive for a post-chemotherapy follow-up of 6-12 months. Tumors relapsed in 5 of 10 (50%) mice treated with 2 mg/kg and in 3 of 10 (30%) treated with 3.5 mg/kg at six months, whereas all animals treated with 5 mg/kg were disease-free after a 12-month follow-up. Post-chemotherapy, histological and immunohistochemical analysis of relapsed masses exhibited a viable serous adenocarcinoma that preserved the morphology and the main

immunophenotypical characteristics of untreated engrafted tumors.

***In vivo* development of a cisplatin-resistant engrafted tumor model that recapitulates cisplatin primary tumor behavior response is a feasible model for pharmacological drug evaluations.**

The general approach use to obtain the cisplatin-resistant engrafted tumor model is illustrated in **Fig 1C**. OVA1X-implanted mice were initially treated with low doses (2 mg/kg) of cisplatin. When tumors relapsed, they were harvested and implanted in new animals (mouse-to-mouse passage). The process was repeated up to five times by treating tumor-bearing mice with stepwise increasing doses of cisplatin (**Fig 1C**). A progressively shortened time-lag between treatment and tumor relapse was noted for the three independent tumor lines (named OVA1XR-L1, -L2, and -L3) generated after iterative cycles of treatment. Indeed, a shortened time-lag was mainly noted after the third or fourth cycle, and became stabilized (41 ± 6.1 days) subsequently for successive cycles of cisplatin treatment (**Fig 1D,** left). Next, we evaluated the levels of cisplatin tumor resistance by comparative assays of OVA1X and each of the three independent lines of resistant tumors and homogeneous resistance was reproduced with each individual OVA1XR tumors (**Fig 1D,** right). Thus, we selected OVA1XR-L2 for all further experiments, hereafter referred to as OVA1XR. **Fig 1A** demonstrates that OVA1X and OVA1XR both recapitulated the histological and immunohistochemical patterns found in the original patient-derived tumor. Interestingly, a consistent loss of estrogen expression was observed among resistant OVA1XR tumor respect to primary and OVA1X.

Lurbinectedin is effective in the treatment of cisplatin-sensitive and cisplatin-resistant ovarian tumor models.

OVA1X and OVA1XR were orthotopically implanted in mice and when homogeneous tumor sizes (300 to 500 mm^3) were identified at palpation (on Days 60 and 64 for OVA1X and OVA1XR, respectively) animals bearing tumors were randomized to the following groups (n=8-12 mice/group): (i) placebo; (ii) cisplatin (3.5 mg/kg); (iii) lurbinectedin (0.180 mg/kg); and (iv) lurbinectedin+cisplatin (0.180+3.5 mg/kg). On Day 21, cisplatin-sensitive tumor OVA1X experienced reductions of 95.3, 88.3 and 87.2% following the treatment with cisplatin, lurbinectedin and lurbinectedin+cisplatin, respectively (**Fig 2A,** left). Although, as single agents both cisplatin and lurbinectedin had a significant response with respect to the placebo-treated animals, non significant differences were observed among both individual treatments. Likewise, combined lurbinectedin+cisplatin treatment had no additional significant benefit with respect to each individual treatment (lurbinectedin+cisplatin *vs*. cisplatin, *P*=0.15; lurbinectedin+cisplatin *vs.*

lurbinectedin, *P*=0.85).

Fig 2B summarizes the results obtained for treatments of cisplatin-resistant tumor (OVA1XR), showing important differences between both tumors for lurbinectedin-based treatments. Thus, 48.2, 93.6 and 96.7% reductions in tumor weight were recorded following cisplatin, lurbinectedin or lurbinectedin+cisplatin treatments, respectively. Lurbinectedin, as a single therapy was a significantly better response than with cisplatin (*P*=0.003). Notably, the combined lurbinectedin+cisplatin treatment proved to be more active than either drug separately, suggesting a synergistic drug effect (lurbinectedin+cisplatin *vs.* lurbinectedin, *P*=0.022; or *vs.* cisplatin, *P*=0.002).

Histopathological changes were assessed for the different treatments within the tumor as surrounding stromal tissue in both cisplatin-sensitive (**Fig 2A**, right*,* and **Supplementary Table 1)** and cisplatin-resistant tumors (**Fig 2B,** right*,* and **Table 1**). Thus, enlargement of tumor cells, presence of multinucleated giant cells, lymphocytic and histiocytic infiltrates with the presence of hemosiderin and fibrosis, and the scarring of tumoral stroma were observed associated with treatments. Interestingly, cisplatin treatment did not induce morphological changes in the cisplatin-resistant OVA1XR tumors (**Fig 2B).**

To investigate the long-term response a subgroup of treated mice (n=4-6 mice/group) were kept alive post-chemotherapy. Thus, OVA1XR tumor relapse took place over a period of 42 days in all cisplatin-treated mice, whereas in cisplatin-sensitive OVA1X regrowth was found in only one cisplatin-treated mouse after eight months follow-up. At sacrifice of OVA1XR, significant differences were found in the weight and histology of relapsed masses (-*RL*) for lurbinectedin-based treatments compared to the cisplatin-*RL* group (lurbinectedin-*RL vs.* cisplatin-*RL*, *P*=0.0020; or lurbinectedin+cisplatin-*RL vs.* cisplatin-*RL*, *P*=0.0008) (**Fig 2C**, upper). Furthermore, combined lurbinectedin+cisplatin treatment was more active than lurbinectedin monotherapy (*P*=0.046), suggesting a long-term synergistic anti-tumor response for combined therapy. This finding is reinforced by the histology of lurbinectedin+cisplatin-*RL* masses (**Fig 2C**, lower). Together, although our results demonstrated the efficacy of lurbinectedin treatment in the treatment of cisplatin-sensitive and cisplatin-resistant orthotopic engrafted tumor models, it is of note that they also suggest a synergistic effect with cisplatin in cisplatin-resistant OVA1XR.

Histopathological tumor regression criteria are associated with treatment response in cisplatin-sensitive OVA1X and cisplatin-resistant OVA1XR tumors.

Cytotoxic therapy leads to morphological and histopathological changes within tumor tissue as well in the involved stroma. Next, we evaluated histopathological tumor regression, which has been established as the gold standard for the assessment of treatment response in several types of solid

tumors (34-37). **Supplementary Table 1** and **Table 1** show extensive analysis of regression criteria for both OVA1X and OVA1XR, to establish whether they are suitable indicators of treatment response, as described for primary neoadjuvant epithelial ovarian cancer (38). Based on these criteria, a moderate histopathological response was observed in OVA1X for single cisplatin and lurbinectedin treatments, while a good response with respect to regression criteria was found for the combined treatment (**Supplementary Table 1**). Taken together, the tumor response and the histopathological regression criteria were evidence of the relevance of the combined treatment in cisplatin-sensitive OVA1X. In this context, in cisplatin-resistant OVA1XR tumor a good histopathological response was confirmed for the combined lurbinectedin+cisplatin treatment (**Table 1**). Moreover, the relevance of combined treatments was reinforced by the observation that the histopathological response was maintained in relapsed masses (**Table 1**).

Lurbinectedin and cisplatin treatments are synergistic in vivo in A2780-derived tumor xenografts.

The synergism of the combined lurbinectedin+cisplatin treatment was further investigated in mice bearing A2780 xenografted tumors. **Fig 3A** shows the T/C values, defined as the change in tumor volume for each treated (T) and placebo (C) group during the placebo-treated survival period, for mice treated with lurbinectedin, cisplatin or combined lurbinectedin+cisplatin. Animals treated with high cisplatin doses showed the lowest T/C of 55.2% on Day 10, while there was no anti-tumor effect induced by the lurbinectedin single-agent treatment (minimal T/C, 70.8% on Day 4). The combined lurbinectedin+cisplatin treatment produced lower T/C values than the more active agent in this experiment (cisplatin at 6.0 mg/kg). The anti-tumor effect seen on Day 4 (T/C, 39.8%) for the highest dose of the combination (0.180 +6.0 mg/kg; lurbinectedin+cisplatin) increased on subsequent days (T/C, 23.4% on Day 10). On Day 10, lurbinectedin+cisplatin treatment displayed a dose-dependent antitumor effect with median tumor volumes (mm^3) of 572.8, 1074, 1233 and 2199 for animals treated with lurbinectedin+cisplatin at 0.180+6.0, 0.135+4.5, 0.09+3.0 and 0.045+1.5 mg/kg levels, respectively. Applying the median-effect principle to the data gave a Combination Index (CI) of 0.17 (at Fa=0.97), suggesting a synergistic effect of the combination lurbinectedin+cisplatin in ovarian (A2780) xenografted tumors (**Fig 3B** and **Table 2**)

Lurbinectedin -induced tumor response is mediated by antiproliferative and proapoptotic features and causes mitotic catastrophe.

Next, we investigated whether tumor response mechanisms were induced by lurbinectedin associated with antiproliferative and proapoptotic features. Two experimental approaches were used: (i) in A2780-derived subcutaneous tumor xenografts treated with cisplatin, lurbinectedin or combined drugs for 24 or 72 hours; (ii) in cisplatin-sensitive OVA1X and cisplatin-resistant OVA1XR tumors.

We found that 24 hours after treatments of the A2780 xenografts, the anti-phospo-Histone H3 (S10)(H3S10ph) mitosis marker significantly decreased in cisplatin (*P*=0.007), lurbinectedin (*P*=0.002) or combined (*P*<0.001) treatments compared with placebo-treated tumors (**Fig. 4A**). In fact, the decrease was significantly greater for the combined treatment than for each single therapy (lurbinectedin+cisplatin *vs.* lurbinectedin, *P*=0.005; or *vs.* cisplatin, *P*=0.015). Additionally, a proapoptotic effect was associated with lurbinectedin treatments. Thus, a 6.7-fold increase in the number of apoptotic cells (by TUNEL assay) was observed in combined lurbinectedin+cisplatin (*P*=0.013) treatment compared with the placebo group, and 3.0-fold and 3.7-fold increases with respect to cisplatin and lurbinectedin, respectively (**Fig. 4C,** left).

Likewise, antiproliferative and proapoptotic effects were confirmed in both engrafted orthotopic models. In OVA1XR (**Fig. 4B**) all treatments showed a significant decrease in the number of mitoses determined by H3S10ph (cisplatin, *P*=0.007; lurbinectedin, *P*=0.003; lurbinectedin+ cisplatin, *P*<0.001). As a single treatment, lurbinectedin was more effective than cisplatin (*P*=0.044). Combined lurbinectedin+cisplatin treatment significantly diminished the number of mitoses with respect to single lurbinectedin (*P*=0.016) or cisplatin (*P*=0.003) treatment (**Fig. 4B**). This effect was also maintained in relapsed tumor masses (lurbinectedin+cisplatin-*RL vs.* cisplatin-*RL*, *P*=0.005; or *vs.* lurbinectedin, *P*=0.012). Apoptotic drug-induction was assessed in OVA1X and OVA1XR by immunodetection in paraffin-embedded tissues of caspase-3, an early and specific apoptotic marker. In cisplatin-sensitive OVA1X, non-significant differences for the proapoptotic-induced effect were observed for the single treatments (cisplatin, 6.3-fold; lurbinectedin, 7.1-fold; *P*=0.45) (**Fig 4C,** right). Whereas in cisplatin-resistant OVA1XR tumor the strong proapoptotic effect was noted for lurbinectedin (4.2-fold induction relative to the placebo, *P*=0.014; and 2.8-fold with respect to cisplatin, *P*=0.007), cisplatin retaining a moderate capability of inducing apoptosis in OVA1XR tumors (1.5-fold induction relative to placebo, *P*=0.036) (**Fig 4C,** right). We did not analyze apoptosis induction in the combined treatment because the extensive histopathological regression prevents the reliable interpretation of the caspase cleaved apoptosis assay (data not shown).

Finally, we investigated whether lurbinectedin treatments affected the morphology of the mitotic spindle by double immunofluorescence staining with α-tubulin (red staining), a protein localized in the spindle, combined with staining with the mitosis marker histone H3S10ph (green staining) (**Fig 4D** and **Supplementary Fig 1**). Thus, in mitotic cells identified by H3S10ph with vehicle-treated tumors, α-tubulin shows that control cells display normal bipolar mitotic spindles with chromosomes correctly aligned on the metaphase plate. On the other hand, lurbinectedin-treated cells exhibited abnormal mitotic figures, with seriously defective chromosome alignment, and the cells displaying aberrant figures failed to progress through mitosis. The presence of cells displaying aberrant figures was particularly manifested for combined lurbinectedin+cisplatin

treatment, in A2780-derived xenografts and both engrafted orthotopic models (**Fig 4D**).

DISCUSSION

In this work we report the generation and characterization of a serous ovarian cancer model based on orthotopic tumor implantation in nude mice, and its further *in vivo* development as a tumor model of cisplatin resistance. Next, as preclinical models, we demonstrate that lurbinectedin, a new synthetic alkaloid binder to the DNA minor groove, is effective either in the treatment of *cisplatin-sensitive* and c*isplatin-resistant* ovarian tumors. So, our results show that the combination of two compounds that differentially bind the DNA major and minor grooves should be a useful treatment strategy for EOC patients, and suggest its importance for overcoming cisplatin-resistance.

Recent data suggest an overall success rate of 10% for oncology products in clinical development, being one of the reasons attributed to this failure the fact that preclinical models used frequently do not predict clinical results (31). Currently, preclinical *in vivo* drug development is mainly realized in subcutaneous (s.c.) tumor xenografts generated after cell line injection, or in some cases after s.c. engraftment of primary tumor (29, 32, 33), and pure primary orthotopic tumor-based models have rarely been used. Few such tumor models are available: because surgery is often complex, small numbers of mice are used per study, and the models are more expensive (28). Here, we demonstrate that these orthotopic-based pre-clinical ovarian tumor models, which reproduce primary tumor properties, are outstanding resources for the development of new drug therapies. They would also be very valuable for exploring new therapeutic applications for drugs that are currently approved for use in humans, as we recently reported in MSI+ colorectal tumors with enoxacin (39). Thus, assessed chemotherapy responses in cisplatin-sensitive and cisplatin-resistant tumor models that maintain the morphological, histological and genetic characteristics of patients' tumors, including the behavior of the stromal component and the tissue architecture, may improve pre-clinical drug translation to patients.

To overcome cisplatin resistance and reduce the side effects, new agents should have different mechanisms of action and should be non-cross-resistant with platinum (40). Structurally, the DNA duplex gives rise to two well-defined clefts known as the major and minor grooves (25). While the DNA major groove represents a site of attack for cisplatin and many alkylating agents, other anti-tumor drugs such as ecteinascidins, mitomycin C and chromomycin A3 bind to the minor groove (16, 17). Our work with the new synthetic alkaloid lurbirnectedin strongly suggests that strategies based on dual major and minor DNA groove-targeted therapies should be useful for treating cisplatin-resistant/refractory cases of ovarian carcinomas. Further studies in these models will allow a deeper insight into the cooperative mechanism of action among cisplatin and

lubirnectedin, and enable their combined properties with other drugs such olaparib, temozolamide, doxorrubicine, etc. to be evaluated. Although, lurbinectedin is structurally similar to trabectedin (Yondelis®), their important different pharmacokinetics properties identified may lead to novel and/or increased antitumor activity compared with original trabectedin (25, 26).

Our preclinical findings in cisplatin-sensitive OVA1X tumor indicate that lurbinectedin monotherapy treatment could be an active first-line drug on the basis of its similar cisplatin response rates and the related long-term behavior response. However, from the clinical standpoint, certainly, the most relevant preclinical result was the capability of lurbinectedin, either on its own or in combination with cisplatin, to overcome the cisplatin resistance of OVA1XR tumor. Its relevance was underlined by the better response and by the histopathological regression found in OVA1XR treated with lurbinectedin alone or combined with cisplatin, both in short- and long-term experiments. All together, our results indicate that combined lurbinectedin treatment should overcome cisplatin resistance, it being an effective second-line treatment for platinum responder patients as a first-line agent for refractory tumors.

In agreement with previously described in vitro results (25), we showed that the tumor response produced in vivo by lurbinectedin was mediated by an antiproliferative and proapoptotic induction and causes mitotic catastrophe. Previous reports demonstrated common PM01183 (lurbinectedin) effectiveness in the nanomolar range in a panel of representative cell lines of different tumor types, and described that PM01183 (lurbinectedin) and cisplatin acted synergistically when tested in vitro on platinum-resistant cells lines (26). In this work, we demonstrated that lurbinectedin synergizes in vivo with cisplatin treatments, an effect that is mainly observed in cisplatin-resistant OVA1XR tumors. It has been reported that although DNA lesions generated by lurbinectedin are not repaired by nucleotide excision repair (NER), it can interfere with NER, thereby attenuating the repair of specific NER substrates. Thus, lurbinectedin has enhanced activity in cisplatin-resistant cell lines with higher NER activity (26).

Dissemination in EOCs characteristically involves local invasion of pelvic and abdominal organs, and unlike many epithelial cancers, initial dissemination rarely requires the vasculature, although this is often involved in the advanced stages of disease (41). The tumor model presented here, as happens in their original patient, rarely disseminate in mice. Nevertheless, the generation of other orthotopic-based EOCs tumor models reproducing human dissemination patterns should be very useful for investigating drug action in malignant ascitis formation, the characteristic feature of advanced ovarian cancer at diagnosis. In fact, we have developed other engrafted primary EOCs models that mimic in mice human local and distal dissemination behaviors (A. Vidal and A. Villanueva, personal communication).

After neoadjuvant chemotherapy, the residual tumor size in ovarian specimens was the

only histopathological criterion that was significantly associated with treatment and subsequent overall survival. Histopathological responders defined by the absence of residual tumor, scattered solitary tumor cells or a residual tumor of 5 mm or less had a significantly longer survival (38). The size of the residual tumor remaining after debulking surgery is known to be an important prognostic factor (42). Likewise, we demonstrate in both tumor models that the size of the residual masses and the abundance of regressive criteria correlate with response. The strong correlation between our preclinical tumor models and clinical settings in terms of tumor progression and response to chemotherapy, strongly argues in favor of conducting clinical lurbinectedin trials in resistant/refractory epithelial ovarian cancer.

In conclusion, we have demonstrated that lurbinectedin, a drug targeting the minor DNA groove, is active and in vivo synergizes with cisplatin, which targets the major DNA groove, in the treatment of orthotopic cisplatin-sensitive and cisplatin-resistant patient-derived preclinical tumor models. Overall, our results provide solid evidence supporting clinical trials with lurbinectedin alone or in combination with cisplatin in advanced EOCs.

Material and Methods

Drugs and cell lines: Lyophilized lurbinectedin (PM01183) vials (1 mg/ml) were obtained from PharmaMar (Colmenar Viejo, Madrid, Spain) and cisplatin (1 mg/ml) from Ferrer-Farma (Barcelona, Spain). The A2780 human ovarian carcinoma cell line was obtained from the European Collection of Cell Cultures (Salisbury, UK). Cell cultures were grown *in vitro* at 37ºC in a humidified atmosphere of 5% CO_2 in RPMI-1640 (Sigma-Aldrich Co) supplemented with 10% fetal calf serum (FBS).

Animals: Female athymic *nu/nu* mice (Harlan™) between 4 to 6 weeks of age were housed in individually ventilated cages on a 12-hour light-dark cycle at 21-23ºC and 40-60% humidity. Mice were allowed free access to an irradiated diet and sterilized water. All animal protocols were reviewed and approved according to regional Institutional Animal Care and Use Committees.

Primary sample and orthotopic tumor-engrafted in mice: The primary tumor specimen was obtained at Hospital Universitari de Bellvitge (L'Hospitalet de Llobregat, Barcelona, Spain). The study was approved by the Institutional Review Board. Written informed consent was collected from a patient who had not received cisplatin-based chemotherapy. Non-necrotic tissue pieces (*ca*. 2 to 3 mm^3) from resected serous human epithelial ovarian tumor were selected and placed in DMEM (BioWhittaker®) supplemented with 10% FBS and penicillin/streptomycin at room

temperature. Under isofluorane-induced anesthesia, animals were subjected to a lateral laparotomy, their ovaries exposed and tumor pieces anchored to the ovary surface with prolene 7.0 sutures. Tumor growth was monitored 2 to 3 times per week and when the tumor grew, it was harvested, cut into small fragments and transplanted into 2-5 new animals. Engrafted tumors at early mouse passages were cut in 6-8 mm^3 pieces and stored in liquid nitrogen in a solution of 90% FBS and 10% DMSO for subsequent implantation.

Histology and immunohistochemical tumor characterization: The morphology of the primary patient's tumor and of the both engrafted tumors (OVA1X and OVA1XR) was compared by H&E staining in paraffin-embedded sections. Determination of cytokeratin (CK) 7, Ki67, WT1, alpha estrogen and progesterone receptors status by immunohistochemistry, in accordance with the standard clinical protocols of the Department of Pathology (*see* **Fig 1** legend).

***In vivo* establishment of cisplatin-resistant xenografted tumor:** Cisplatin-resistant tumor (named OVA1XR) was developed by iterative cycles of *in vivo* exposure to cisplatin of OVA1X. Briefly, orthotopically engrafted OVA1X tumors (at mouse passage #3) were allowed to grow until intra-abdominal palpable masses were noted. Then, animals were intravenously (i.v.) administered with cisplatin at a dose of 2 mg/kg for 3 consecutive weeks (Days 0, 7 and 14) (cycle#1 of treatment). Post-cisplatin tumor relapse were harvested, prepared as previously described, and engrafted in new animals. This process was repeated up to five times by treating tumor-bearing mice with stepwise increasing doses of cisplatin: cycle#2, 3 mg/kg; cycle#3, 3.5 mg/kg; cycle#4, 4 mg/kg; and cycle#5, 5 mg/kg (*see* **Fig 1C**). Cisplatin-resistant tumors were obtained in three independent experiments (OVA1XR-L1, -L2 and -L3). At doses higher than 3.5 mg/kg, signs of cisplatin-induced toxicity were ameliorated by 2 days administration of saline containing 5% glucose.

Drug treatment of engrafted cisplatin-sensitive and cisplatin-resistant tumor models: Mice were transplanted with fragments of OVAX1 and OVAX1R tumors, and when tumors reached a homogeneous palpable size were randomly allocated into the treatment groups (n=8-12/group): i) Placebo; ii) Lurbinectedin (0.18 mg/kg); iii) Cisplatin (3.5 mg/kg); and, iv) Lurbinectedin plus cisplatin (0.18+3.5 mg/kg). Drugs were intravenously administered once per week for three consecutive weeks (Days 0, 7 and 14). Seven days after the final dose (Day 21), animals were sacrificed, their ovaries dissected out and weighed. Representative fragments were either frozen in nitrogen or fixed and then processed for paraffin embedding.

Evaluation of histological response after chemotherapeutic treatment: Regressive

histopathological features were evaluated (43-46), and three histological response categories were established (38): (i) *NHR*, no histopathological response (≤1 regression criterion [3+] present); (ii) *MHR*, moderate (2 regression criteria [3+] present); and (iii) *GHR*, good histopathological response (≥ 3 regression criteria [3+] present).

***In vivo* evaluation of synergism among lurbinectedin and cisplatin treatments:** Female mice were subcutaneously implanted with 10^7 A2780 cells suspended in a 1:1 solution of RPMI-1640:Matrigel™ (Becton, Dickinson & Co.). Mice bearing tumors (*ca*. 150 mm^3) were randomly allocated to 13 treatment groups (*see* **Fig 3** legend). All treatments were intravenously administered once per week for two consecutive weeks (Days 0 and 7). Tumor growth was recorded 2-3 times per week starting from the first day of treatment (Day 0) and tumor volume (in mm^3), estimated according to the formula $V=(a \cdot b^2)/2$, (*a*: length or biggest diameter; *b*: width or smallest diameter). Antitumor drug activity was measured with respect to the T/C index, and the fraction affected (F_a) by treatment was calculated (F_a=1-T/C). A combination index (CI) was determined by the CI-isobol method (47).

Determination of tumor proliferation, apoptosis and angiogenesis: Proliferation was assessed by quantifying the anti-phospo-Histone H3 (S10) (Millipore) mitosis marker as described (48). Aberrant mitotic figures were identified by double immunostaining with α-tubulin (1:200) and anti-phospo-Histone H3 (S10) (48). Apoptotic cells were quantified with two approaches: (i) immunostaining in paraffin-embedded samples with anti-Cleaved Caspase-3 (Asp175) antibody (Cell Signaling) at 1:200; and (ii) by terminal deoxynucleotidyl transferase-mediated biotin-dUTP nick end labeling (TUNEL) staining kit (Promega) in frozen OCT tissues (49).

Statistical analysis: Post-chemotherapy tumor weight data were analyzed using a two-tailed Mann-Whitney *U* test. The data are presented as medians and interquartile ranges (IQRs) or means ± standard deviations. Statistical analyses were done and graphs plotted using GraphPad Prism, version 5.02 (GraphPad Software Inc., San Diego, USA). Synergism analyses were done by CompuSyn, version 1.0 (ComboSyn Inc., Paramus, NJ, USA).

Acknowledgements

This work was supported in part by grants FIS PI10-0222 (A.V) and Centro para el Desarrollo Tecnológico e Industrial (CDTI) IDI-20101640. A.Vidal received a BAE grant (BAE/00073) from the Instituto de Salud Carlos III. DH is a Ramon y Cajal Researcher; CM is an AGAUR Fellow and FJG was supported by FIS.

Disclosure of potential conflicts of interest

A. Villanueva has received a Research Grant from PharmaMar, SA.

M.J. Guillén, C. Cuevas and P. Avilés are employees and shareholders of PharmaMar, SA (Madrid, Spain).

Bibliography

1. Jemal A, Siegel R, Ward E, Murray T, Xu J, Thun MJ. Cancer statistics, 2007. CA Cancer J Clin 2007;57:43-66.
2. Alberts DS, Liu PY, Hannigan EV, O'Toole R, Williams SD, Young JA, et al. Intraperitoneal cisplatin plus intravenous cyclophosphamide versus intravenous cisplatin plus intravenous cyclophosphamide for stage III ovarian cancer. N Engl J Med 1996; 335:1950-5.
3. Armstrong DK, Bundy B, Wenzel L, Huang HQ, Baergen R, Lele S, et al. Intraperitoneal cisplatin and paclitaxel in ovarian cancer. N Engl J Med 2006;354:34-43.
4. Berkenblit A, Cannistra SA. Advances in the management of epithelial ovarian cancer. J Reprod Med 2005;50:426-38.
5. Bhoola S, Hoskins WJ. Diagnosis and management of epithelial ovarian cancer. Obstet Gynecol 2006;107:1399-410.
6. Hoskins WJ, Bundy BN, Thigpen JT, Omura GA. The influence of cytoreductive surgery on recurrence-free interval and survival in small-volume stage III epithelial ovarian cancer: a Gynecologic Oncology Group study. Gynecol Oncol 1992;47:159-66.
7. Muggia FM, Hainsworth JD, Jeffers S, Miller P, Groshen S, Tan M, et al. J. Phase II study of liposomal doxorubicin in refractory ovarian cancer: antitumor activity and toxicity modification by liposomal encapsulation. J Clin Oncol 1997;15:987-93.
8. Lund B, Hansen OP, Theilade K, Hansen M, Neijt JP. Phase II study of gemcitabine (2',2'-difluorodeoxycytidine) in previously treated ovarian cancer patients. J Natl Cancer Inst 1994;86:1530-3.
9. ten Bokkel Huinink W, Gore M, Carmichael J, Gordon A, Malfetano J, Hudson I, et al. Topotecan versus paclitaxel for the treatment of recurrent epithelial ovarian cancer. J Clin Oncol 1997;15:2183-93.
10. Rothenberg ML, Liu PY, Wilczynski S, Nahhas WA, Winakur GL, Jiang CS, et al. Phase II trial of vinorelbine for relapsed ovarian cancer: a Southwest Oncology Group study. Gynecol Oncol 2004;95:506-12.
11. Poveda, A. Introduction. Trabectedin treatment in GYN cancers. Int J Gynecol Cancer 2011;21 Suppl 1:S1-2.
12. Gonzalez-Martin AJ, Calvo E, Bover I, Rubio MJ, Arcusa A, Casado A, et al. Randomized phase II trial of carboplatin versus paclitaxel and carboplatin in platinum-sensitive recurrent advanced ovarian carcinoma: a GEICO (Grupo Español de Investigación en Cáncer de Ovario) study. Ann Oncol 2005;16:749-55.
13. Pujade-Lauraine E, Wagner U, Aavall-Lundqvist E, Gebski V, Heywood M, Vasey PA, et al. Pegylated liposomal Doxorubicin and Carboplatin compared with Paclitaxel and Carboplatin for patients with platinum-sensitive ovarian cancer in late relapse. J Clin Oncol 2010;28:3323-9.

14. Alberts DS, Liu PY, Wilczynski SP, Clouser MC, Lopez AM, Michelin DP, et al. Randomized trial of pegylated liposomal doxorubicin (PLD) plus carboplatin versus carboplatin in platinum-sensitive (PS) patients with recurrent epithelial ovarian or peritoneal carcinoma after failure of initial platinum-based chemotherapy (Southwest Oncology Group Protocol S0200). Gynecol Oncol 2008;108:90-4.
15. Ushijima K. Treatment for recurrent ovarian cancer-at first relapse. J Oncol 2010;2010:497429.
16. Pabo CO, Sauer RT. Protein-DNA recognition. Annu Rev Biochem 1984;53:293-321.
17. Rohs R, West SM, Sosinsky A, Liu P, Mann RS, Honig B. The role of DNA shape in protein-DNA recognition. Nature 2009;461:1248-53.
18. Susbielle G, Blattes R, Brevet V, Monod C, Kas E. Target practice: aiming at satellite repeats with DNA minor groove binders. Curr Med Chem Anticancer Agents 2005;5:409-20.
19. Guan Y, Sakai R, Rinehart KL, Wang AH. Molecular and crystal structures of ecteinascidins: potent antitumor compounds from the Caribbean tunicate Ecteinascidia turbinata. J Biomol Struct Dyn 1993;10:793-818.
20. Kishi K, Yazawa K, Takahashi K, Mikami Y, Arai T. Structure-activity relationships of saframycins. J Antibiot (Tokyo) 1984;37:847-52.
21. Pommier Y, Kohlhagen G, Bailly C, Waring M, Mazumder A, Kohn KW. DNA sequence- and structure-selective alkylation of guanine N2 in the DNA minor groove by ecteinascidin 743, a potent antitumor compound from the Caribbean tunicate Ecteinascidia turbinata. Biochemistry 1996;35:13303-9.
22. Casado JA, Rio P, Marco E, Garcia-Hernandez V, Domingo A, Perez L, et al. Relevance of the Fanconi anemia pathway in the response of human cells to trabectedin. Mol Cancer Ther 2008;7:1309-18.
23. Manzanares I, Cuevas C, Garcia-Nieto R, Marco E, Gago F. Advances in the chemistry and pharmacology of ecteinascidins, a promising new class of anti-cancer agents. Curr Med Chem Anticancer Agents 2001;1:257-76.
24. Bueren-Calabuig JA, Giraudon C, Galmarini CM, Egly JM, Gago F. Temperature-induced melting of double-stranded DNA in the absence and presence of covalently bonded antitumour drugs: insight from molecular dynamics simulations. Nucleic Acids Res 2011;39:8248-57.
25. Leal JF, Martinez-Diez M, Garcia-Hernandez V, Moneo V, Domingo A, Bueren-Calabuig et al. PM01183, a new DNA minor groove covalent binder with potent in vitro and in vivo anti-tumour activity. Br J Pharmacol 2010;161:1099-110.
26. Soares DG, Machado MS, Rocca CJ, Poindessous V, Ouaret D, Sarasin A, et al. Trabectedin and its C subunit modified analogue PM01183 attenuate nucleotide excision repair and show activity toward platinum-resistant cells. Mol Cancer Ther 2010;10:1481-9.

27. de Plater L, Lauge A, Guyader C, Poupon MF, Assayag F, de Cremoux P, et al. Establishment and characterisation of a new breast cancer xenograft obtained from a woman carrying a germline BRCA2 mutation. Br J Cancer 2010;103:1192-200.
28. Teicher BA. Tumor models for efficacy determination. Mol Cancer Ther 2006;5:2435-43.
29. Bibby MC. Orthotopic models of cancer for preclinical drug evaluation: advantages and disadvantages. Eur J Cancer 2004;40:852-7.
30. Derose YS, Wang G, Lin YC, Bernard PS, Buys SS, Ebbert MT, et al. Tumor grafts derived from women with breast cancer authentically reflect tumor pathology, growth, metastasis and disease outcomes. Nat Med 2011;17:1514-20.
31. Hait WN. Anticancer drug development: the grand challenges. Nat Rev Drug Discov 2010;9:253-4.
32. Kerbel RS. Human tumor xenografts as predictive preclinical models for anticancer drug activity in humans: better than commonly perceived-but they can be improved. Cancer Biol Ther 2003;2:S134-9.
33. Teicher BA, Herman TS, Holden SA, Wang YY, Pfeffer MR, Crawford JW, et al. Tumor resistance to alkylating agents conferred by mechanisms operative only in vivo. Science 1990;247:1457-61.
34. Evans DB, Rich TA, Byrd DR, Cleary KR, Connelly JH, Levin B, et al. Preoperative chemoradiation and pancreaticoduodenectomy for adenocarcinoma of the pancreas. Arch Surg 1992;127:1335-9.
35. Honkoop AH, Pinedo HM, De Jong JS, Verheul HM, Linn SC, Hoekman K, et al. Effects of chemotherapy on pathologic and biologic characteristics of locally advanced breast cancer. Am J Clin Pathol 1997;107:211-8.
36. Junker K, Thomas M, Schulmann K, Klinke F, Bosse U, Muller KM. Tumour regression in non-small-cell lung cancer following neoadjuvant therapy. Histological assessment. J Cancer Res Clin Oncol 1997;123:469-77.
37. Mandard AM, Dalibard F, Mandard JC, Marnay J, Henry-Amar M, Petiot JF, et al. Pathologic assessment of tumor regression after preoperative chemoradiotherapy of esophageal carcinoma. Clinicopathologic correlations. Cancer 1994;73:2680-6.
38. Sassen S, Schmalfeldt B, Avril N, Kuhn W, Busch R, Hofler H, et al. Histopathologic assessment of tumor regression after neoadjuvant chemotherapy in advanced-stage ovarian cancer. Hum Pathol 2007;38:926-34.
39. Melo S, Villanueva A, Moutinho C, Davalos V, Spizzo R, Ivan C, et al. Small molecule enoxacin is a cancer-specific growth inhibitor that acts by enhancing TAR RNA-binding protein 2-mediated microRNA processing. Proc Natl Acad Sci U S A 2011;108:4394-9.
40. Dunton CJ. New options for the treatment of advanced ovarian cancer. Semin Oncol 1997;24:S5-2-S5-11.

41. Shield K, Ackland ML, Ahmed N,cRice GE. Multicellular spheroids in ovarian cancer metastases: Biology and pathology. Gynecol Oncol 2009;113:143-8.
42. Cannistra SA. Cancer of the ovary. N Engl J Med 2004;351:2519-29.
43. Becker K, Mueller JD, Schulmacher C, Ott K, Fink U, Busch R, et al. Histomorphology and grading of regression in gastric carcinoma treated with neoadjuvant chemotherapy. Cancer 2003;98:1521-30.
44. Fisher ER, Wang J, Bryant J, Fisher B, Mamounas E, Wolmark N. Pathobiology of preoperative chemotherapy: findings from the National Surgical Adjuvant Breast and Bowel (NSABP) protocol B-18. Cancer 2002;95:681-95.
45. McCluggage WG, Lyness RW, Atkinson RJ, Dobbs SP, Harley I, McClelland HR, et al. Morphological effects of chemotherapy on ovarian carcinoma. J Clin Pathol 2002;55:27-31.
46. Moreno A, Escobedo A, Benito E, Serra JM, Guma A, Riu F. Pathologic changes related to CMF primary chemotherapy in breast cancer. Pathological evaluation of response predicts clinical outcome. Breast Cancer Res Treat 2002;75:119-25.
47. Chou TC, Talalay P. Quantitative analysis of dose-effect relationships: the combined effects of multiple drugs or enzyme inhibitors. Adv Enzyme Regul 1984;22:27-55.
48. Huertas D, Soler M, Moreto J, Villanueva A, Martinez A, Vidal A, et al. Antitumor activity of a small-molecule inhibitor of the histone kinase Haspin. Oncogene 2012;31:1408-18.
49. Castillo-Avila W, Piulats JM, Garcia Del Muro X, Vidal A, Condom E, Casanovas O, et al. Sunitinib inhibits tumor growth and synergizes with cisplatin in orthotopic models of cisplatin-sensitive and cisplatin-resistant human testicular germ cell tumors. Clin Cancer Res 2009;15:3384-95.

Figure Legends

Figure 1 Establishment, and comparative histopathological characterization of primary and engrafted OVA1X and its paired developed cisplatin-resistant OVA1XR tumor. **A)** Upper, lateral laparatomy was performed in isofluorane-anesthetized mice, the ovary mobilized and small tumor pieces of primary tumor anchored on the ovarian mouse surface with prolene 7.0 sutures. Engrafted tumors grew as large solid masses (usually 1000-1500 mm^3) in diameter at the time of sacrifice, and ovarian infiltration/invasion or ascitis were not seen. Lower, representative H&E and immunohistochemical staining reveals a high correlation between primary and paired engrafted tumors. Primary antibodies were monoclonal antibodies: CK7 (clone OV-TL 12/30, Dako); Ki67 (clone MIB-1, Dako); WT1 (clone 6F-H2, Dako) and estrogen receptor alpha (clone SP1, Dako) OV, ovary; TL, tumor engrafted in the left ovarian; TD, engrafted in the right ovarian; UT, uterus. **B)** Mice engrafted with OVA1X tumor were treated intravenously with low (2 mg/kg), intermediate (3.5 mg/kg) and high (5 mg/kg) cisplatin doses, and either short- or long-term responses were analyzed for each treatment. For short-term response studies, all dose-response mice were sacrificed on Day 21 after treatment, while for long-term studies they were sacrificed after six months. **C)** Experimental approach used for cisplatin-resistant tumor generation combines: (i) iterative cycles of cisplatin treatment (three doses of cisplatin administered by i.v. injection on Days 0, 7 and 15); and (ii) successive increase of administered doses through the process. **D)** Left, illustrates a short time-lag between succesive cycles of treatment for three independent OVA1XR-L1, -L2 and -L3 tumor lines. For each line, tumors at cycle #5 of cisplatin treatment (arrow), were selected for further cisplatin assays. Right, shows comparative short-time cisplatin response between untreated OVA1X tumor *vs.* each independent cisplatin-resistant OVA1XR-L1, -L2 and -L3 tumors. All mice were treated with 2 mg/kg of cisplatin administered by i.v. injection on Days 0, 7 and 15 and sacrificed on Day 21. *, $P<0.05$.

Figure 2 Response of engrafted OVA1X and OVA1XR tumors after lurbinectedin-based chemotherapy treatments. Animals were treated with placebo, cisplatin (3.5 mg/kg) or lurbinectedin (0.180 mg/kg) administered following the same schedule in three doses by i.v. tail vein injection on Days 0, 7 and 15 and sacrificed on Day 21 (n=8 placebo; n=10 cisplatin; n=12 lurbinectedin; and n=12 combined lurbinectedin+cisplatin treatments). The doses of the combination (0.180 mg/kg + 3.5 mg/kg; lurbinectedin plus cisplatin) were selected on the basis of the optimal treatment tolerability in mice bearing tumors (data not shown). **A** and **B)** Graphs illustrate responses of cisplatin-sensitive OVA1X and cisplatin-resistant OV1XR tumors on Day 21 of treatment. Histopathological characterization of residual tumor masses post-chemotherapy of cisplatin-sensitive OVA1X and cisplatin-resistant OVA1XR tumors, respectively. Sections were stained with H&E and an extensive study of tumor regression characteristics done, as an indicator

of chemotherapeutic response (*see* **Supplementary Table 1** and **Table 1**). **C)** Characterization of the long-term response of cisplatin-resistant OVA1XR tumor. A subgroup of mice (n=5) for each treatment were kept alive post-chemotherapy, and were simultaneously sacrificed upon tumor relapse of the cisplatin-treated group. The graph illustrates differences in the weight of relapsed tumor masses for the different treatments. Histopathological characterization of relapsed tumor masses (-*RL*) from mice treated with cisplatin, lurbinectedin and lurbinectedin+cisplatin. Sections were stained with H&E and an extensive study of tumor regression characteristics done, as an indicator of chemotherapeutic response (see Supplementary Table 1 and Table 2). cisplatin-*RL*, lurbinectedin-*RL*, lurbinectedin+cisplatin-*RL*, tumor relapsed after cisplatin, lurbinectedin or combined treatments, respectively. *, $P<0.05$.

Figure 3 *In vivo* characterization of the synergistic effect among lurbinectedin and cisplatin treatments. Xenografted subcutaneous tumor were generated in nude mice after injection of 10^7 cells of the A2780 ovarian cancer cell line, and mice bearing tumors (*ca*. 150 mm^3) were randomly allocated to 13 treatment groups (n=8-10/group): i) placebo; ii) lurbinectedin at four dose levels, namely MTD (0.180 mg/kg), 0.75 MTD (0.135 mg/kg), 0.5 MTD (0.09 mg/kg) and 0.25 MTD (0.045 mg/kg); iii) cisplatin, at four dose levels MTD (6 mg/kg), 0.75 MTD (4.5 mg/kg), 0.5 MTD (3.0 mg/kg) and 0.25 MTD (1.5 mg/kg); and, iv) lurbinectedin plus cisplatin, administered with the combination at (1+1), (0.75+0.75), (0.50+0.50) and (0.25+0.25) of MTD ratios. **A)** Graphs show antitumor activity of each single or combined treatment followed by T/C values, defined as the change in tumor volume for each treated (T) and placebo (C) group during the placebo-treated survival period. **B)** Determination of tumor fraction affected (F_a) by treatment, calculated according to the formula F_a=1-T/C and combination index (CI) determined by the CI-isobol method using CompuSyn software, version 1.0 (ComboSyn, Inc. Paramus, NJ, USA).

Figure 4 Tumor proliferation was determined after immunostaining mitotic figures with anti-phosphorylated histone H3 (S10) antibody (H3S10ph) (green staining), and mitotic spindles with anti α-tubulin (red staining). Chromosomes were labeled with DAPI in the blue channel. Treatment doses were: i) lurbinectedin (0.18 mg/kg); ii) cisplatin (3.5 mg/kg); and, iii) lurbinectedin plus cisplatin (0.18 + 3.5 mg/kg). **A)** In A2780-derived subcutaneous tumors (A2780X) and **B)** in residual tumor masses of cisplatin-resistant OVA1XR tumor or in long-term relapsed masses (-RL)(36 Days after the sacrifice of the short-term response group). Stained cells were counted in six non-overlapping representative fields. Images were taken with a Leica TCS LP5 spectral confocal microscope (Leica Microsystems) with 20X and 63X objectives and 405 Diode, Argon and DPSS 561 lasers, acquiring stacks every 1 mm. Stacks were projected and processed using ImageJ software (MacBiophotonics). Hotspot fields in viable comparable tissues zones at x400

magnification were captured for each tumor and quantified, also taking the stromal component into consideration. **C)** Apoptosis was evaluated by TUNEL and immunostaining of Caspase 3. Left, TUNEL assay in A2780X subcutaneous tumors treated with lurbinectedin, cisplatin or combined lurbinectedin+cisplatin, and mice sacrificed 72 h post-treatment. Right, cleaved Caspase 3 was analyzed in paraffin sections of residual tumor masses on Day 21 of single cisplatin and lurbinectedin treatments of OVA1X and OVA1XR tumors. **D)** The presence of aberrant mitotic figures was determined by co-immunostaining with anti-H3S10ph and anti-α-tubulin (48) in A2780X subcutaneous tumors 72 h post-treatment as in residual masses of OVA1X and OVA1XR tumors on Day 21 of treatment. Graphs show the percentage of aberrant mitosis in OVA1X tumor. Scale bar is 10 μm. *, $P<0.05$.

Author Manuscript Published OnlineFirst on August 15, 2012; DOI:10.1158/1078-0432.CCR-12-1513
Author manuscripts have been peer reviewed and accepted for publication but have not yet been edited.

Figure 1

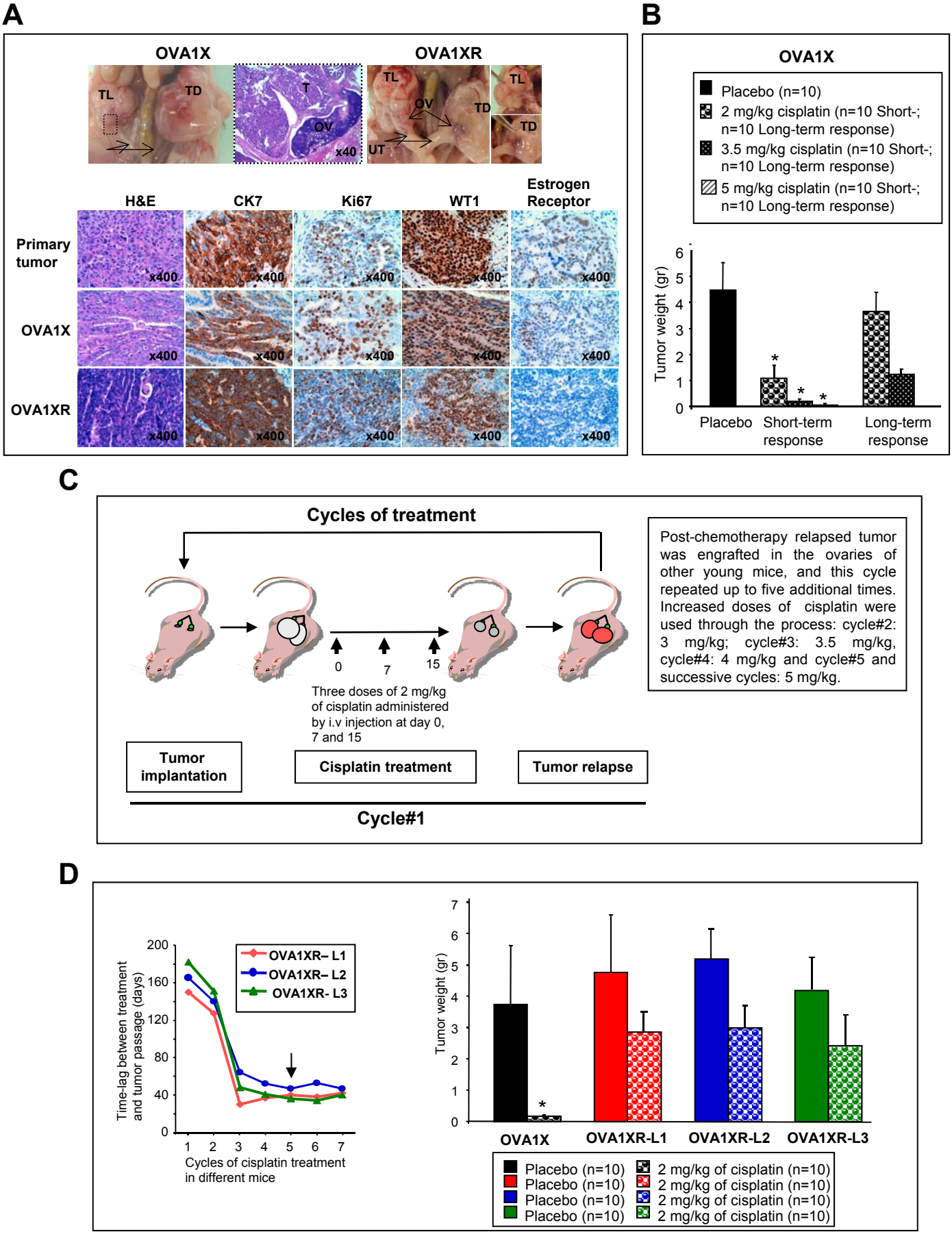

Figure 2

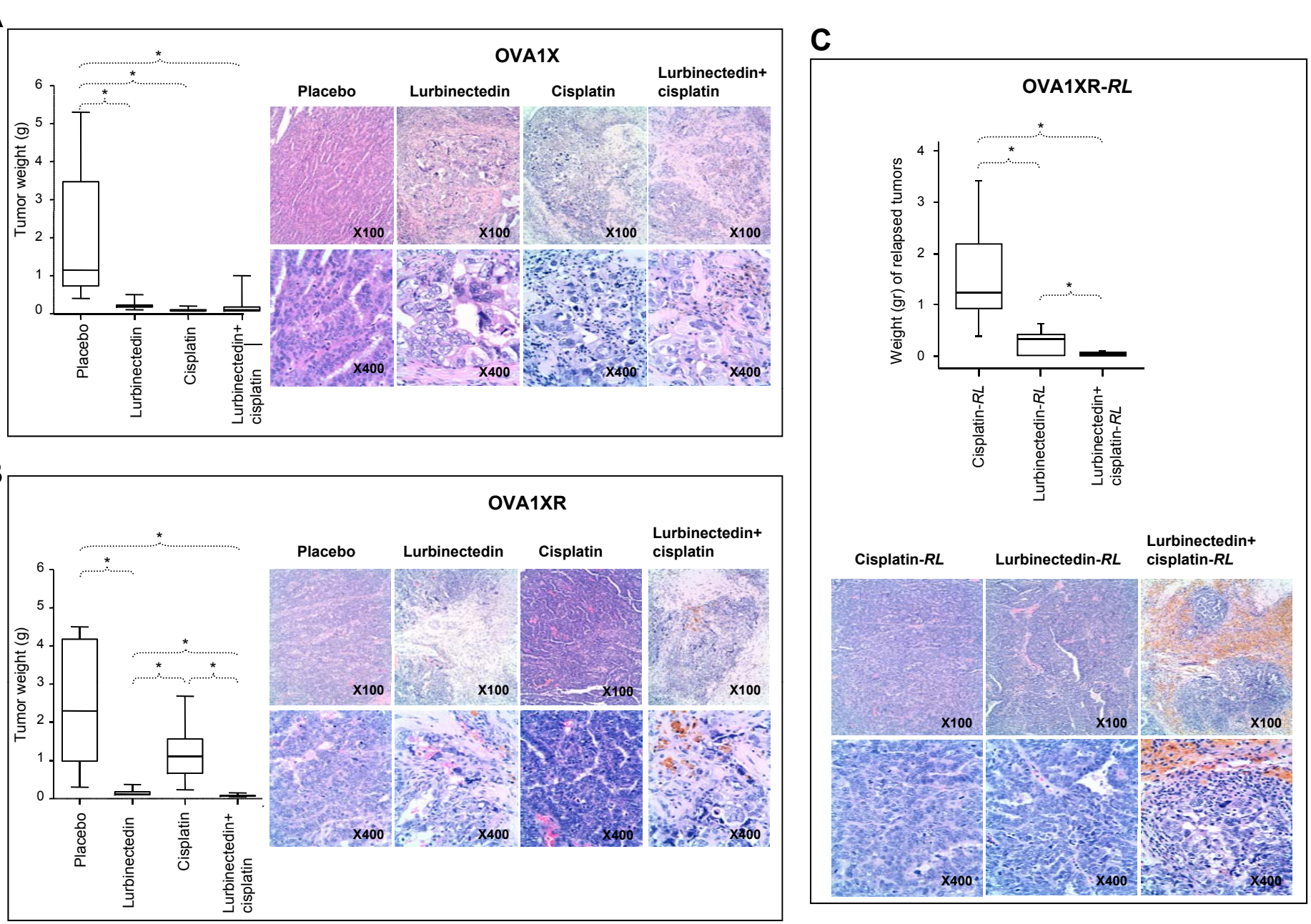

Author Manuscript Published OnlineFirst on August 15, 2012; DOI:10.1158/1078-0432.CCR-12-1513
Author manuscripts have been peer reviewed and accepted for publication but have not yet been edited.

Figure 3

A

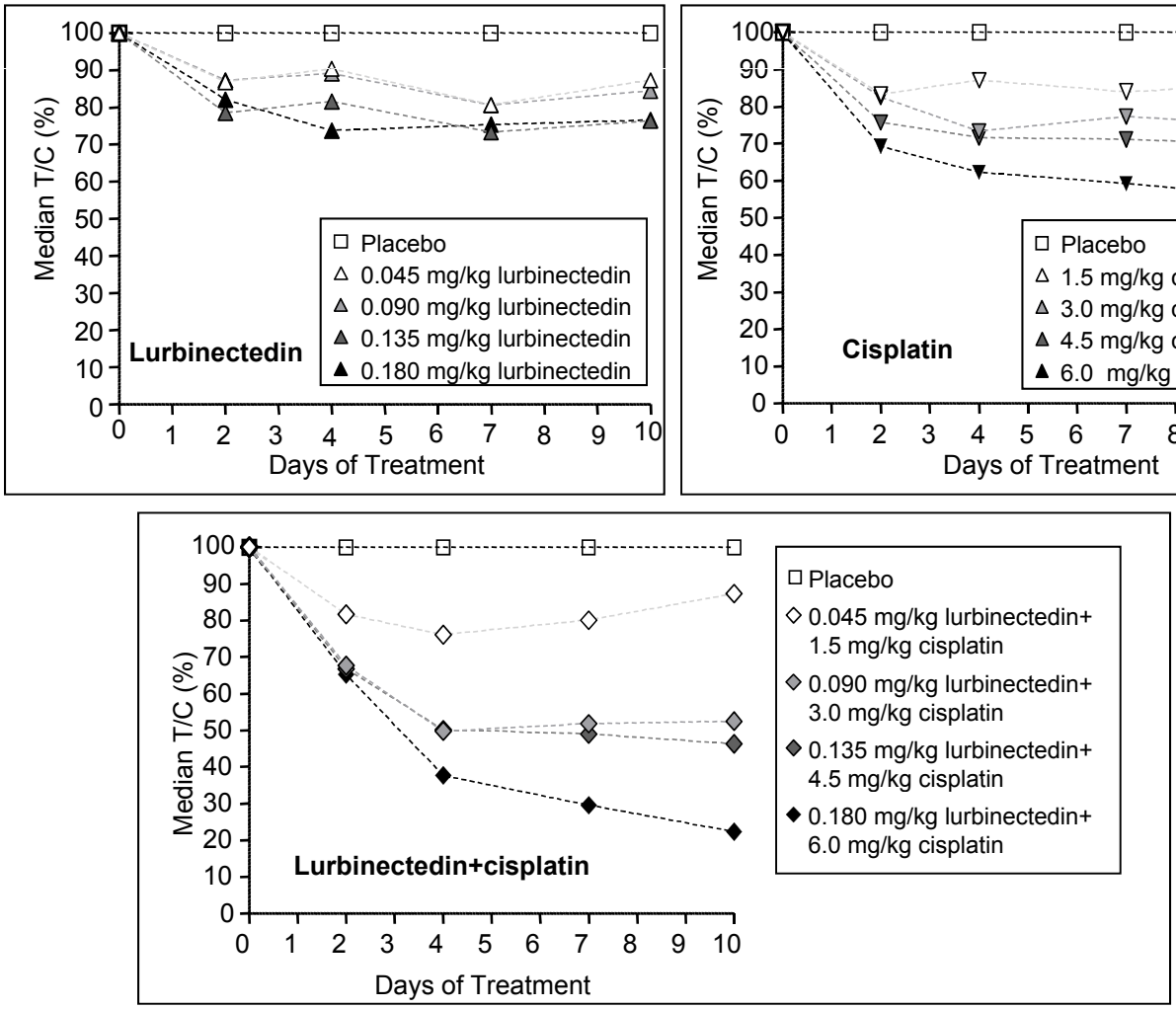

B

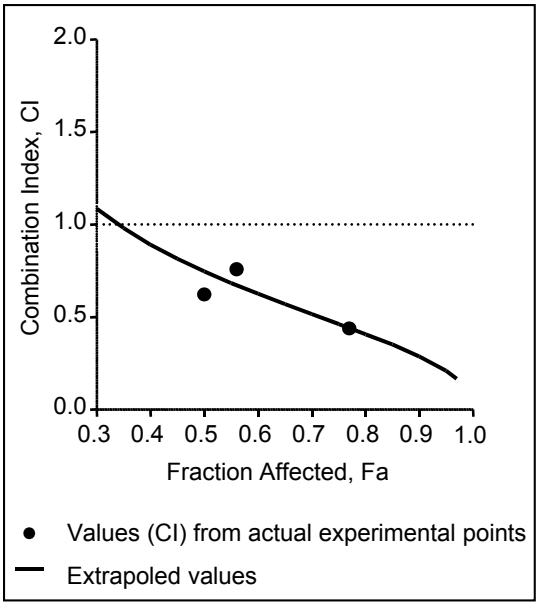

Figure 4

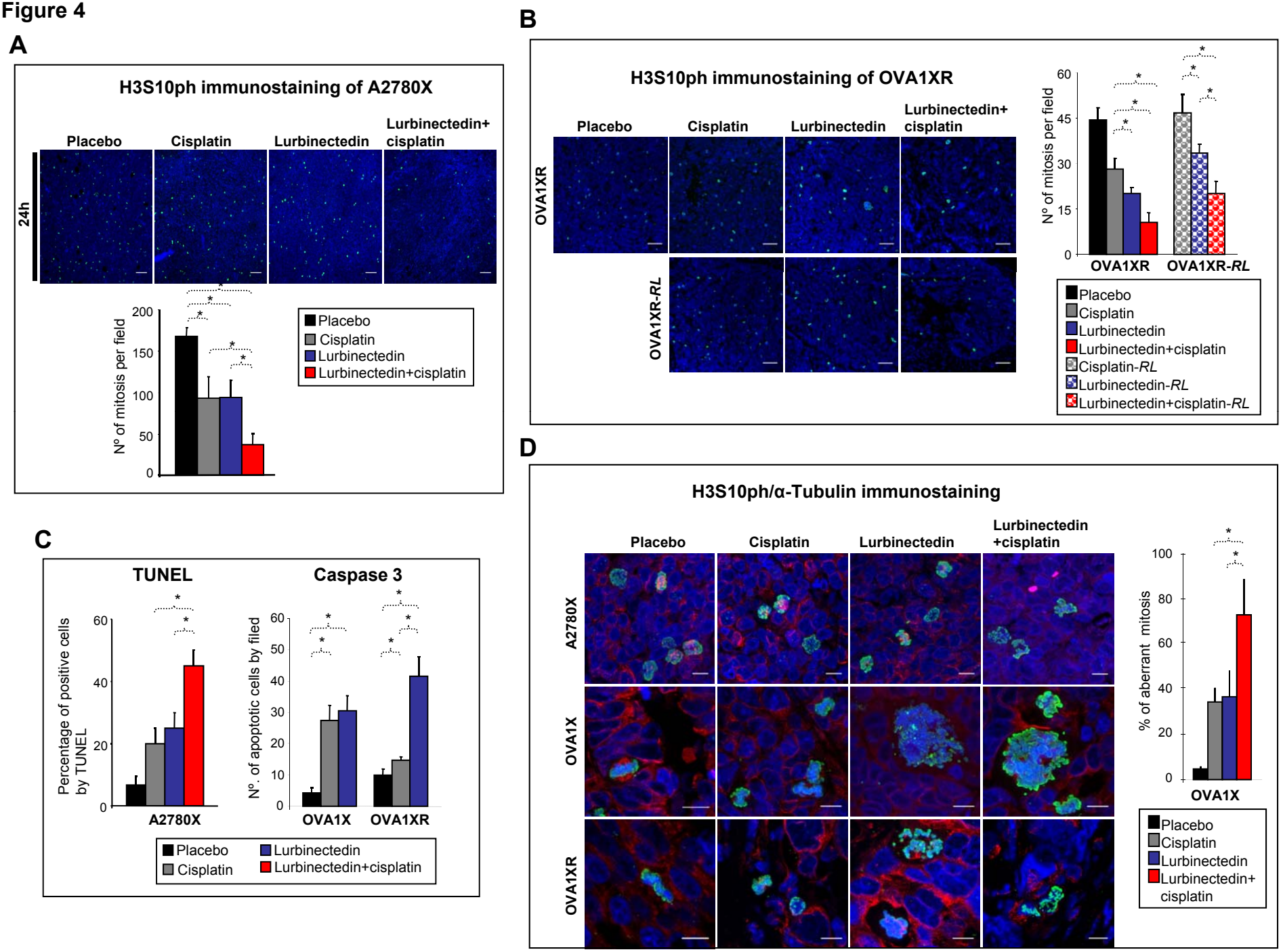

Table 1 Extensive histopathological tumor regression criteria analyses in post-chemotherapy engrafted OVA1XR tumor.

	Mice	Fibrosis	Necrosis	Inflammation	Foamy macrophages	Calcification	Hemosiderin	Foreign-body giant cells	Giant tumor cells	Pattern of tumor infiltration [b]	Chemotherapy response based on histopathological features [e]
Short-term response [a]											
Placebo	1	0	1+	0	0	0	0	0	1+	1+	*NHR*
	2	0	1+	1+	0	0	0	0	1+	1+	*NHR*
	3	1+	1+	0	0	CD [c]	0	0	1+	1+	*NHR*
	4	1+	0	1+	0	0	0	0	1+	1+	*NHR*
	5	1+	1+	0	0	0	0	0	1+	1+	*NHR*
Cisplatin	6	2+	0	0	0	0	0	0	0	1+	*NHR*
	7	2+	0	0	0	0	1+	0	1+	1+	*NHR*
	8	1+	0	0	0	0	1+	0	1+	1+	*NHR*
	9	1+	0	0	0	0	0	0	1+	1+	*NHR*
	10	1+	1+	0	0	0	0	0	1+	1+	*NHR*
Lurbinectedin	11	2+	1+	1+	0	0	2+	0	2+	2+	*NHR*
	12	2+	0	1+	0	CD	2+	0	2+	2+	*NHR*
	13	2+	0	2+	0	0	2+	0	2+	2+	*NHR*
	14	1+	0	1+	0	0	1+	0	1+	1+	*NHR*
	15	2+		1+	0	0	2+	0	2+	1+	*NHR*
Lurbinectedin+cisplatin	16	3+	0	2+	0	0	2+	0	3+	2+	*MHR*
	17	3+	0	1+	0	0	2+	0	3+	3+	*GHR*
	18	3+	0	2+	0	CD	2+	0	3+	3+	*GHR*
	19	1+	0	2+	0	0	1+	0	3+	3+	*MHR*
	20	3+	0	1+	1+	CD	2+	0	3+	3+	*GHR*
Long-term response [a]											
Cisplatin-RL	21	1+	1+	0	0	0	0	0	1+	1+	*NHR*
	22	1+	2+	1+	0	0	0	0	1+	1+	*NHR*
	23	1+	0	0	0	0	0	0	1+	1+	*NHR*
Lurbinectedin-RL	24	1+	0	1+	0	0	1+	0	1+	1+	*NHR*
	25	1+	0	1+	0	0	0	0	1+	1+	*NHR*
	26	3+	0	1+	0	0	2+	0	3+	2+	*MHR*
	27	NV [d]	NV	NV	NV	NV	NV	NV	NV	NV	*GHR*
Lurbinectedin+cisplatin-RL	28	3+	0	2+	0	0	2+	0	3+	3+	*GHR*
	29	3+	0	1+	0	0	0	0	3+	3+	*GHR*
	30	NV	NV	NV	NV	NV	NV	NV	NV	NV	*GHR*
	31	NV	NV	NV	NV	NV	NV	NV	NV	NV	*GHR*

[a] For short-term response studies, animals were sacrificed on day 21 of treatment, while for long term-response studies, mice were sacrificed 42 days after the end of treatment when the tumor had relapsed.

[b] Pattern and extent of tumor infiltration was classified as follows: 1+, macroscopic large confluent tumor mass(es); 2+, multiple small tumor foci; 3+, scattered solitary tumor cells or complete absence of residual tumor. The remaining regression criteria were graded as follows: 0/1+, no or only minimally presence of the regression criterion within the specimen; 2+, focal occurrence of the respective regression criterion; 3+, widespread occurrence of the respective regression criterion.

[c] CD, Dystrophic Calcification.

[d] NV, Not evaluated by complete tumor regression. Characterized by the absence of macro- and microscopic lesions.
[e] Three histopathological response categories were defined based on the number of regression criteria: *NHR*, no histopathological response (≤ 1 regression criteria [3+] present); *MHR*, moderate (2 regression criteria [3+] present), and *GHR*, good histopathological response (≥3 regression criteria [3+] present).

Table 2 Dose-response treatment effect of subcutaneous xenografts of A2780-derived cell line.

Treatment	Dose (mg/kg)	Fraction affected [a] (F_a)	Dose-effect parameters [b]		
			m **(SD)**	**D_m**	***r***
Lurbinectedin	0.180	0.29	1.04 (0.16)	2.12	0.978
	0.135	0.26			
	0.090	0.22			
	0.045	0.09			
Cisplatin	6.0	0.45	1.24 (0.12)	1.29	0.990
	4.5	0.31			
	3.0	0.23			
	1.5	0.12			
Lurbinectedin+cisplatin	0.180+6.0	0.77	2.34 (0.36)	1.20	0.977
	0.135+4.5	0.56			
	0.090+3.0	0.50			
	0.045+1.5	0.10			

[a] Fraction affected (F_a=1-T/C), defined as the change in tumor volume for each treated (*T*) and placebo (*C*) groups during placebo-treated survival period.

[b] Derived from the median-effect plot: [logFa/(1-Fa)] *vs*. log(Dose), where *m* is the slope (as mean±SD), D_m is the intercept of the plot, and *r* is the linear regression coefficient